

See discussions, stats, and author profiles for this publication at: <https://www.researchgate.net/publication/353527687>

Beamforming of Broadband Rotor Noise

Conference Paper · August 2021

DOI: 10.2514/6.2021-2189

CITATIONS

0

READS

69

7 authors, including:



Christopher Hickling

Virginia Tech (Virginia Polytechnic Institute and State University)

15 PUBLICATIONS 124 CITATIONS

SEE PROFILE



N. Agastya Balantrapu

University of Utah

13 PUBLICATIONS 63 CITATIONS

SEE PROFILE



Jarrod Banks

Virginia Tech (Virginia Polytechnic Institute and State University)

7 PUBLICATIONS 9 CITATIONS

SEE PROFILE



Humza Butt

Virginia Tech (Virginia Polytechnic Institute and State University)

7 PUBLICATIONS 9 CITATIONS

SEE PROFILE



Beamforming of Broadband Rotor Noise

Stewart A. L. Glegg,¹

Florida Atlantic University, Boca Raton FL 33431

W. Nathan Alexander², Christopher Hickling³, Agastya Balantrapu², Jarrod Banks² Humza Butt², and William Devenport⁴

Virginia Tech, Blacksburg VA 24060

Abstract

This paper considers the beamforming of rotor noise from a large microphone array in a wind tunnel with a high level of background noise and shows how the array measurements for a single focus point can be compared with the beamformed spectra obtained using a rotor noise prediction code. Using this approach the tunnel background noise, which was dominated by high levels of machinery noise, could be separated from the rotor noise source levels. The parameters needed to populate the prediction model are then optimized so that it is applicable at all angles and ranges from the source in spite of the poor signal to noise ratio in the test environment.

I. Introduction

Beamforming methods for broadband rotor noise are frequently used when measurements are made in a noisy environment, such as a wind tunnel, so that the signal to noise ratio is enhanced. The approach is to use the output of a microphone array to create a source image of the rotor, and then use an integration of the image in the area of the rotor, with a correction for the point spread function, to obtain the source level at a particular frequency. The source image integration method was first used by Glegg [1] in 1979 and is described in detail by Dougherty [2]. However, array beamforming methods assume that the sources being measured are omnidirectional which is never the case for rotor noise, and so the integrated beamform maps do not define a Source Level (SL). By definition the SL is the far field sound level, corrected for inverse spreading to a reference distance from the source, in the direction of the maximum in the source directivity. At best, a microphone array, using delay and sum beamforming and corrected using any type of deconvolution method, will give an average of the source level and the directivity function, which must be less than the true source level. There is also no guarantee of self-consistency, which by definition requires that the same source level is obtained regardless of the array design used. To some extent this problem can be overcome by using the generalized polar correlation method, Fisher *et al.* [3], in which beamforming is based on the cross spectrum between a reference microphone and the other microphones in the array. This gives the source level as seen by the reference microphone, Glegg [4], but the point spread function obtained using this approach does not produce as sharp of an image as would be obtained using a standard delay and sum approach. However, in noisy wind tunnel environments, this is not necessarily the biggest problem. The primary difficulty is caused by the source directivity because, at radiation angles where there are low levels from the source of interest, the signal to noise ratio can be prohibitively low. As we will show below, more accurate results can often be obtained by eliminating microphones at locations where the source signal is expected to be negligible compared to the background noise. This correction, however, is frequency dependent, and this leads to a further lack of robustness.

¹ Professor, Department of Ocean and Mechanical Engineering, Associate Fellow AIAA.

² Assistant Professor, Center for Renewable Energy and Aero/hydrodynamic Technology, Kevin T. Crofton Department of Aerospace and Ocean Engineering, Member AIAA.

³ Graduate Research Assistant, Center for Renewable Energy and Aero/hydrodynamic Technology, Kevin T. Crofton Department of Aerospace and Ocean Engineering.

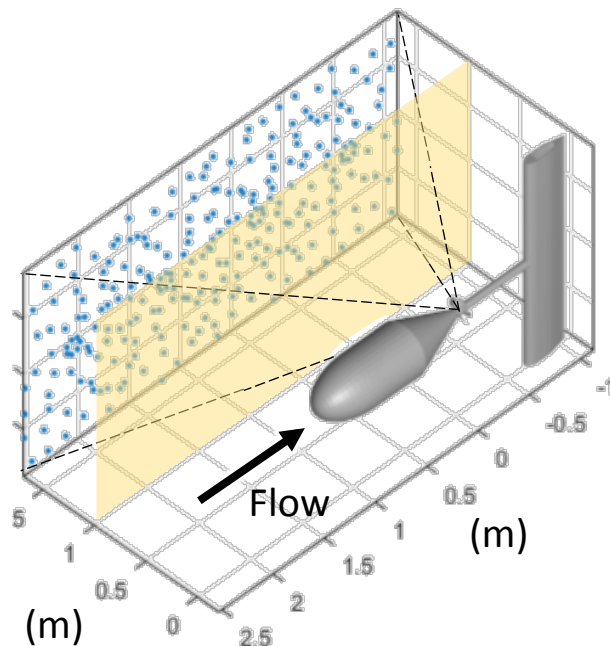
⁴ Professor, Center for Renewable Energy and Aero/hydrodynamic Technology, Kevin T. Crofton Department of Aerospace and Ocean Engineering, Associate Fellow AIAA.

An alternative approach, which is described in this paper, is to beamform onto a single point at, say, the center of the rotor, and to present the results as a function of frequency compared to the spectrum that would be predicted using a rotor noise prediction method. The simplest of models for the source would be a dipole with its axis coincident with the axis of the rotor, but much more accurate or realistic results can be obtained from a more sophisticated rotor noise prediction model. The parameters that determine the predicted levels, such as the force spectrum, or the turbulence intensities and lengthscales of the rotor inflow, can then be adjusted to match the measured spectra. Once these are known then the level at any microphone in the array, or any other point in the far field, can be calculated from the rotor noise model, which of course is the purpose of the measurement in the first place.

In the following sections we will show the results from using this approach for rotor noise measurements in a wind tunnel environment using a 251 element microphone array as described in Hickling et al [5]. This data set was subject to very high levels of background noise and so provides a good test of the approach.

II. Beamforming Measurements

The rotor noise measurements took place in the Virginia Tech Stability Wind Tunnel and are fully described in [5]. A rotor was operated over a range of speeds in the wind tunnel with a nominal axial inflow velocity of 20 m/s and the experimental arrangement shown in Figure 1. The rotor has five blades and a diameter of 216 mm and the upstream body has maximum diameter of 432 mm and overall length of 1.37 m. The details of the rotor and the mounting system and drive are shown in [5] and will not be repeated here.



a)



b)

Figure 1: (a) The experimental arrangement and (b) the microphone array in the Virginia Tech Stability Wind Tunnel.

The acoustic measurements were made using a 251 element microphone array, shown in Figure 1, with elements in both the forward and rear arc of the rotor. This array is composed of four similarly sized, interwoven spiral sub-arrays centered at different streamwise locations in the tunnel. For this study, only data from the second most downstream spiral, will be presented. The microphones in this sub-array extend from a location 1.194 m upstream of the rotor disc plane to a location 0.418 m downstream of the rotor disc plane. The rotor drive system was the dominant source of background noise, which exceeded the rotor noise levels in the rear arc and included periodic components that caused tones at the shaft rotation frequency that were 15dB above the broadband noise level at certain frequencies as shown in Figure 2.

To extract the rotor noise source level from the background noise the traditional approach [1,2] is to use the output from each microphone in the array to obtain a beamformed map of the source region as illustrated in Figure 3 (for an ideal rotor with no noise added). The source level is then obtained by integrating the beamformed map over the source region to get the total source strength, with a correction applied for the point spread function, or resolution of the array. The beamform map only applies at one frequency and so the beamformed maps at each frequency must be integrated to get a source spectrum.

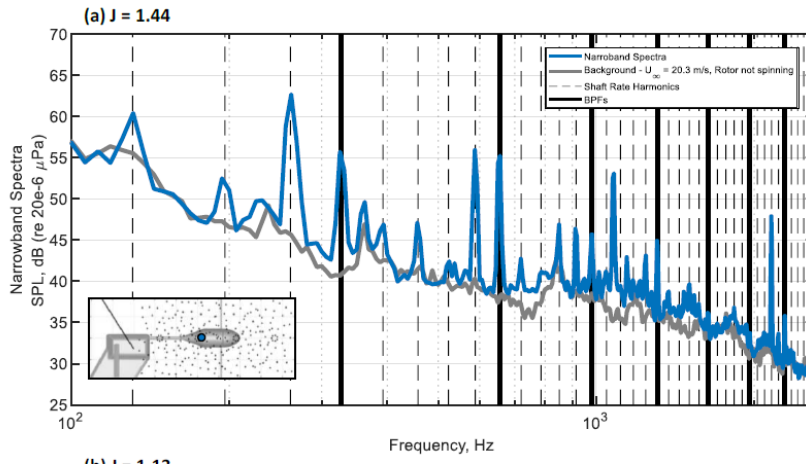


Figure 2: The signal to noise ratio for a single microphone measurement for the BOR test.

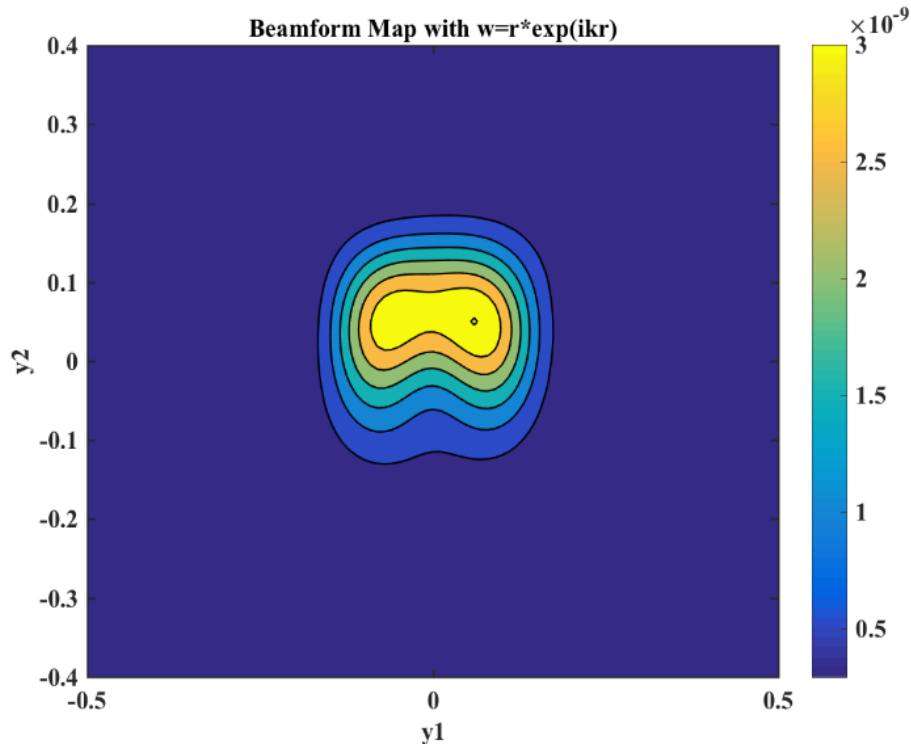


Figure 3: An example of a beamformed map for an idealized rotor. The source level as a function of position in the rotor disc plane is shown for a single frequency.

While this is an accepted approach [1,2] it does not account for the source directionality, which for rotor noise sources can be significant. The problem caused by directionality is illustrated in Figure 4, which shows a schematic of a rotor and a near field microphone array, as used in a wind tunnel environment. It is clear from this illustration

that parts of the array have a very low signal to noise because the source directionality causes a very small signal level.

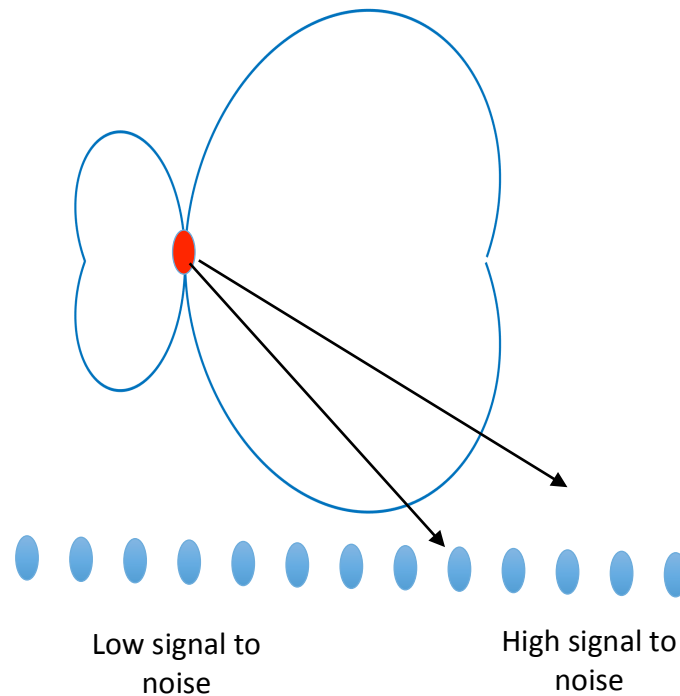


Figure 4: The effect of source directionality on each microphone in the array

One approach to improve the results is to only use the signals from those microphones in the array where the signal to noise level is expected to be large enough to give a good result. This requires using a select set of sensors or a sub array, but this also has the effect of reducing the spatial resolution of the source image and the number of microphones used to process the data, which causes a corresponding reduction in signal to noise. Another alternative is to use the coherence cross spectral matrix rather than the cross spectral matrix to form the source image [4]. Beamforming the coherence normalizes the output of each microphone by its spectral level and so makes the source appear omnidirectional. However this also has the effect of amplifying the lower level signals in comparison to the higher level signals, and so can also worsen the noise distortion of the source image.

The one feature of this measurement that is known with a high level of accuracy is the location of the source, and so the use of a "source location" method is redundant. The issue is extracting the "source level" in a poor signal to noise environment. For the case of a rotor at very low frequencies a simple model of the source is the axial component of unsteady rotor loading and can be characterized by a force spectrum $S_{FF}(f)$ and a cosine directionality with a peak along the axis of the rotor. To characterize this source we only need to measure the force spectrum. Then in any design application the acoustic far field can be predicted because both the source level and the directionality are known. This simplistic model can also give a prediction of the cross spectral density matrix of a microphone array in the near or far field as a function of the force spectrum and so, if we match the predicted cross spectrum with the measured cross spectrum with a suitable weighting for each element in the array, we can obtain a least squares estimate of the force spectrum.

The key to the success of this approach is obviously the weighting used in the least squares estimate, but this should maximize the output of the array relative to the extraneous noise for the source at the known source point. This is obviously achieved by taking the array output that is focused on the source location. In that case the signal from the source is maximized compared to the signal from the background noise.

The rotor noise source, especially at high frequencies and for tip Mach numbers that are not negligible, is far more complex than the simple axial force model discussed above. The directionality will be a function of frequency and cannot be characterized by a simple dipole source. However the approach described above can still be used if a more accurate rotor noise prediction model is used. Typical rotor noise models will have a number of input parameters, which will include the details of the rotor inflow and turbulence, and can be used to predict the array output for any arrangement of near or far field sensors. The approach is therefore to find the correct set of model input parameters that gives the best fit to the far field microphone array data.

Regions of poor signal to noise in the microphone array will obviously reduce the accuracy of this approach. However, the accuracy of the measurement is not dependent on the spatial resolution of the source image, but on the number of sensors used to fit the model. The best signal to noise ratio will be obtained from the microphones with the best signal to noise, and adding signals with poor SNR will reduce the accuracy of the result. The results should be independent of the array used and so a good measure of the accuracy of the source model is to compare the differences between the predicted and measured levels for different sub arrays. The sub arrays where the error between the predicted level and measurement is inconsistent with other sub array outputs can be identified as having low SNR, or the far/near field locations where the source model is unreliable.

Of course, the rotor noise prediction model used in this approach must be accurate. For this series of tests, a time domain based approach was used which has previously been shown to give accurate results [7]. However this approach is not limited to the use of a single model and any suitable alternative can be used.

III. The Prediction Model

As described above, the approach to beamforming this data set was based on the concept of comparing the beamformed spectra for an image point at the center of the rotor with the predicted beamformed spectra using the same set of microphones and array processing method. The noise predictions are based on the time domain rotor noise code described by Glegg *et al.* [6] and verified against benchmark data in Glegg *et al.* [7]. This formulation predicts the far field noise based on the correlation function of the force applied to the fluid by each blade section and requires the evaluation of the multiple integrals and summations given by the prediction formula

$$C_{pp}(\mathbf{x}^{(j)}, \mathbf{x}^{(k)}, \omega) = \frac{1}{4\pi T} \sum_{n=1}^B \sum_{m=1}^B \int_{R_{\min}}^{R_{\max}} \int_{R_{\min}}^{R_{\max}} \int_{-T}^T \int_{-T}^T R_{FF}^{(n,m)}(R, R', \tau, \tau') \times \left\{ \frac{\partial}{\partial x_i} \frac{n_i^{(n)}(R, \tau) e^{i\omega r^{(n,j)}(R, \tau)/c_o}}{4\pi r^{(n,k)}(R, \tau)} \right\} \left\{ \frac{\partial}{\partial x_i} \frac{n_j^{(m)}(R', \tau') e^{-i\omega r^{(m,k)}(R', \tau')/c_o}}{4\pi r^{(m,k)}(R', \tau')} \right\} e^{i\omega(\tau-\tau')} dR dR' d\tau d\tau' \quad (1)$$

In this formula $C_{pp}(\mathbf{x}^{(j)}, \mathbf{x}^{(k)}, \omega)$ is the cross spectral density between the observer locations at $\mathbf{x}^{(j)}$ and $\mathbf{x}^{(k)}$, for the frequency ω , $R_{FF}(R, R', \tau, \tau')$ is the cross correlation of the unsteady blade loading at radii R and R' for times τ and τ' . The propagation distance from the blade section at radius R for the time τ for the n^{th} blade to the observer location $\mathbf{x}^{(j)}$ is given by $r^{(n,j)}(R, \tau)$ and the blade normal for the n^{th} blade at radius R for the time τ is given by $n_i^{(n)}(R, \tau)$. This formulation is greatly simplified for axisymmetric inflow, as was the case in this study, because the unsteady load is independent of blade location and only a function of $\tau - \tau'$.

To obtain the unsteady loading correlation function a time domain formulation is given that specifies

$$R_{FF}^{(n,m)}(R, R', \tau, \tau') = \int_{-\infty}^{\tau} \int_{-\infty}^{\tau'} s(R, \tau - \tau'_o) s(R', \tau' - \tau'_o) R_{ww}^{(n,m)}(R, R', \tau_o, \tau'_o) d\tau_o d\tau'_o \quad (2)$$

where $s(R, \tau)$ is the Sear response function in the time domain for an upwash gust with a time history $w(R, \tau)$ at the leading edge of each blade section, and $R_{ww}^{(n,m)}(R, R', \tau, \tau')$ is its correlation between blade sections and between each blade.

This model requires the definition of the inflow turbulence at the rotor face and these were based on RANS calculations of the turbulence kinetic energy (Perry [8]), and assumed a Liepmann correlation function with axis dependent lengthscales. Figure 5 shows the estimated average upwash velocity and good agreement with measurements is seen.

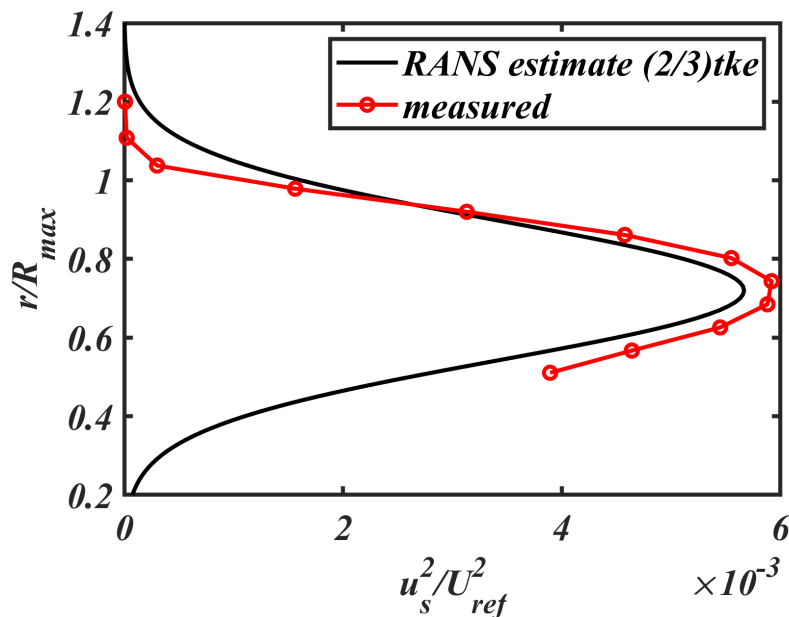


Figure 5: The distribution of turbulence intensity estimated from RANS calculation of the flow in the wake of the BOR compared to measurements, taken from Perry [8].

In Figure 6, the correlation function for the Liepmann model is shown as a function of time delay and displacement along a circumferential arc in the rotor plane (see equation 9.1.27 and 9.1.28 in [9]). In this model the axial and circumferential lengthscales were taken to be unequal which rotates the axis of the correlation function in the time/space domain as shown in Figure 6. This skewing of the correlation function causes hystacking and right shifting of the peaks close to blade passing frequency in the far field spectra as will be discussed below.

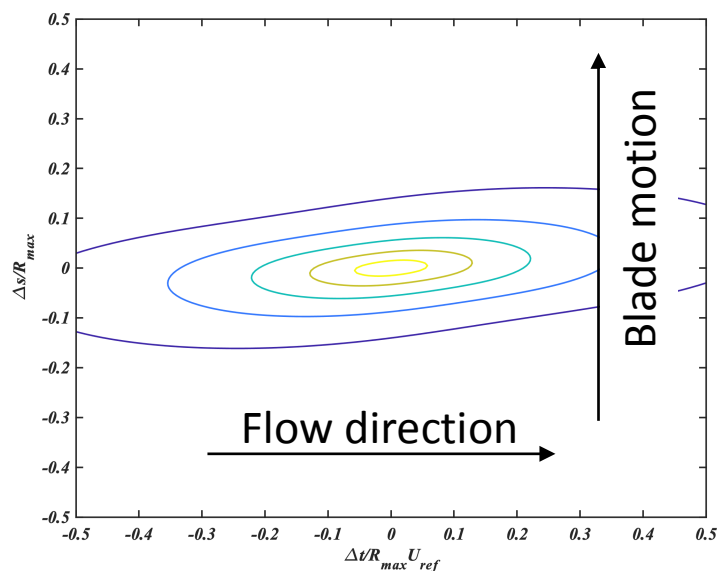


Figure 6: The correlation function based on the Liepmann model used in the calculation. Δs is a displacement along a circumferential arc (see Figure 7) and Δt is the time delay between measurements at a fixed point.

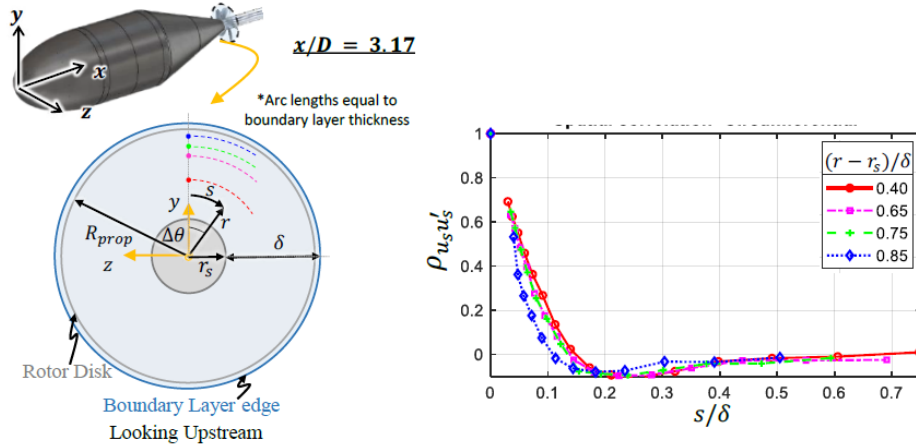


Figure 7: The measured correlation of the axial component of the turbulent velocity in the wake of the BOR as a function of azimuthal displacement at a fixed rotor radius.

Figure 7 shows the measured correlation function in the wake of the BOR as a function of azimuthal separation. This appears to be consistent with radial displacement. In Table 1, the lengthscales are given for each radial location, where L_x is the axial lengthscale and L_c is the circumferential lengthscales. The Liepmann model used in the acoustic prediction code is compared to the measured correlation function in Figure 8

R/R_{max}	L/R_{max}	L_c/R_{max}	L_x/L_c
0.59	0.114	0.044	2.58
0.77	0.112	0.41	2.74
0.85	0.107	0.41	2.65
0.92	0.099	0.032	3.1

Table 1: The measured axial and circumferential lengthscales in the wake of the BOR. BOR Diameter $D=0.4318$ m, Wake thickness $\delta=0.0798$ m, $R_{max}=0.10795=D/4$.

The axial flow lengthscales used to plot the predicted curves in Figure 8 were found to be larger than the lengthscales obtained from the measurements, but this is consistent with the larger negative parts of the curves in the measured data that tends to reduce the integral lengthscales. Using the larger estimated values gives a better fit to the data near the peaks in the correlation function, which is consistent with the requirements for the acoustic prediction code. The estimated lengthscales used in Figure 8 are $L_c=0.06 R_{max}$ and $L_x=1.9L_c$.

One of the advantages of the approach given by the method described above is that, for an axisymmetric turbulent inflow, the evaluation of equation (1) is fast enough to compute the full cross spectral density matrix, at all frequencies and for all 251 microphones, in a few minutes. The predicted CSM matrix can then be analyzed using the same array processing algorithm as applied to the measured data and a direct comparison between the two can be made.

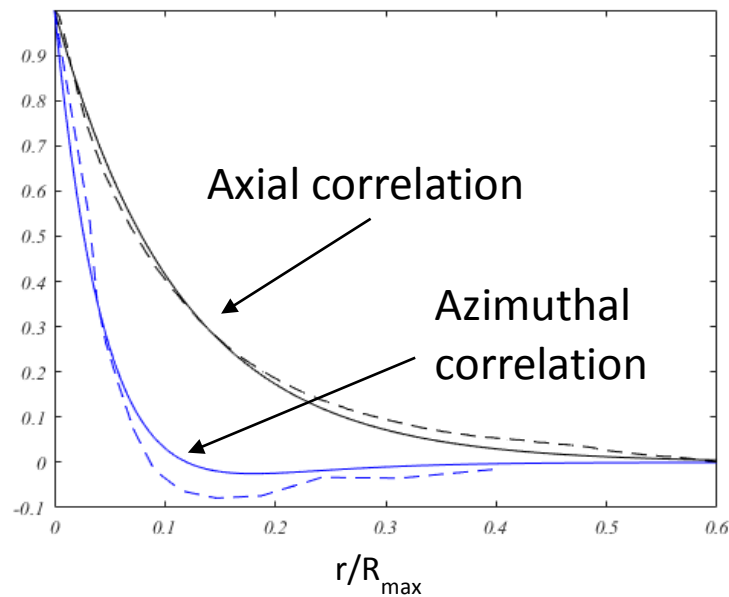


Figure 8: The modeled and measured correlation functions a function of radial displacement with $L_c=0.06R_{max}$ and $L_x=1.9L_w$ compared to measurements (dashed lines).

IV. Beamforming Results

To illustrate the results we will first consider the spectral level from a single microphone at 60° to the rotor axis is shown in Figure 9. For this measurement, the rotor was spinning at 3926 RPM with a 20 m/s inflow corresponding to a condition of zero mean thrust. Note the very high tone levels that were caused by the rotor drive system. Also shown is the spectrum obtained when the array outputs are beamformed for a focus point at the center of the rotor using an array of 51 microphones in the forward arc. This sub-array was defined as all the microphones that were in front of the rotor disc plane and so includes some sensors in the region of the far field where the rotor noise is a minimum. The lower level that is obtained demonstrates the effective reduction of the tunnel background noise that can be achieved by beamforming, especially at high frequencies.

One of the issues with beamforming in a wind tunnel is the effect of shear layer refraction. This causes two effects. The first is the change in propagation time for the furthest upstream microphones which are closest to the axis of the wind tunnel. The wave propagation upstream is slowed by the wind tunnel flow and so this must be allowed for in the beamforming algorithm. The additional delay causes an additional phase shift which was found to be as much as 38° at 12 bpf. However the maximum phase error at 4 bpf is only 10° . The effect that this has on the beamformed spectra is shown in Figure 10. Clearly at frequencies above 5 bpf the shear layer refraction correction increases the beamformed levels. However, in addition to the change in propagation distance there is also the effect of phase scrambling by the turbulent boundary layer on the wind tunnel walls. This will add a fluctuation in propagation time, that must be less than the turbulence intensity, and will be most pronounced for the upstream microphones. For these reasons we have chosen to only present data for frequencies below 5 bpf since these are least affected by refraction and shear layer turbulence.

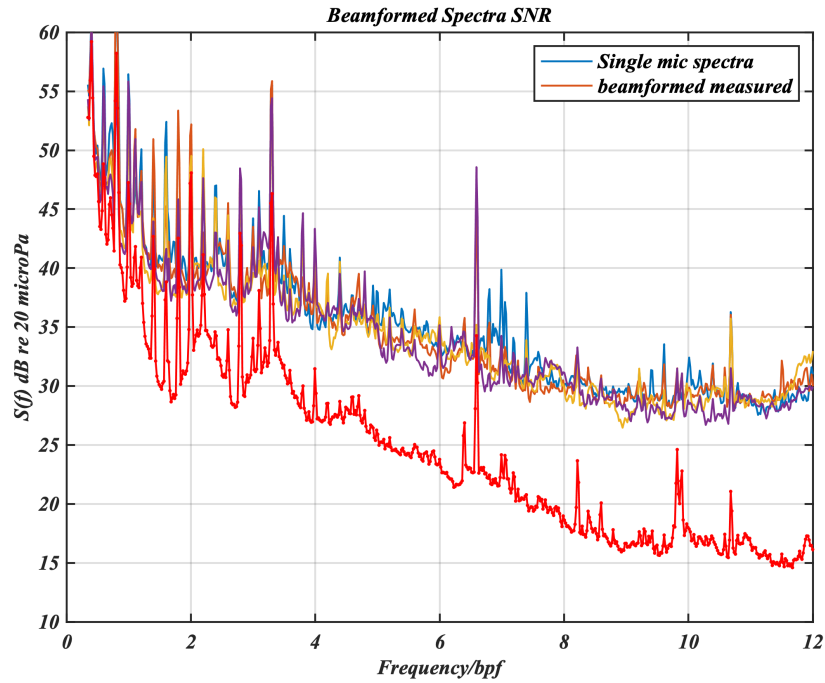


Figure 9: The spectra measured using a single microphone compared to the beamformed spectra as a function of frequency re the blade passing frequency.

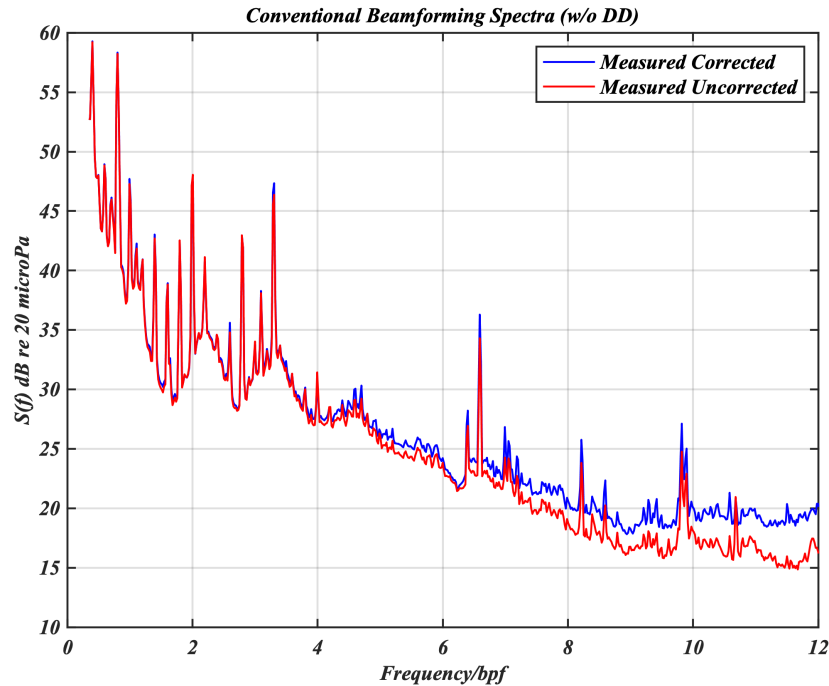


Figure 10: Beamformed spectra with and without corrections for shear layer refraction spectra as a function of frequency re the blade passing frequency.

The beamformed spectra are compared to the rotor noise prediction model in Figure 11. To generate this result the rotor inflow turbulence levels were based on the measured correlation functions as described above, and only the 51 microphones in front of the rotor disc plane were used in the beamforming. It appears that the prediction method does quite a good job over this frequency range in estimating the measured broadband noise levels to within 3 dB over the frequency range shown, apart from at frequencies that are less than blade passing frequency, where one would expect the background noise to dominate. However the tone levels generated by the rotor drive system are still the dominant part of the measured spectra, and the details of the broadband noise spectral shape are not matched. The measured broadband spectra has a well-defined pattern with humps that are typical of haystacking peaking just above 2 and 3 bpf.

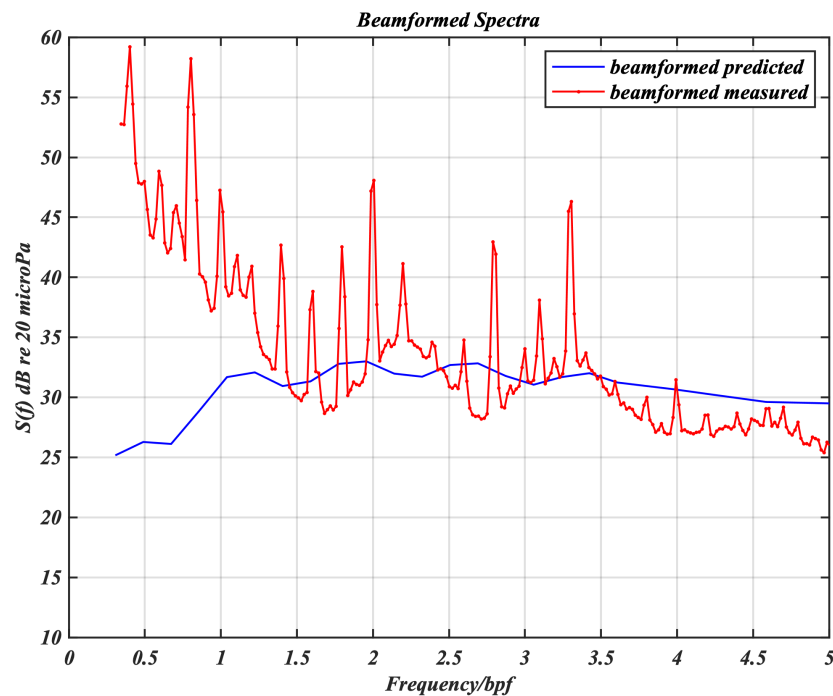


Figure 11: The beamformed spectral levels from the array microphones in the forward arc using delay and sum beamforming for array of 51 microphones.

To improve the spectral fit the prediction model was run with the revised lengthscales of $L_c=0.06 R_{max}$ and $L_x=4L_c$. These were optimized to give the best fit to the acoustic data and the results are shown in Figure 12. For the broadband noise level the agreement between the measurement and the model is greatly improved (with the exception of the tone levels as would be expected). The spectral humps have the correct level, but close to 2 bpf the peak frequency of the haystack is not correctly predicted.

The conclusion from this is that the lengthscales measured just upstream of the rotor appear to be about half the lengthscales required to achieve the optimum fit to the acoustic data. Whether there is a physical explanation for this remains to be seen as more information about the rotor inflow is processed. However, as far as the measurement of the source level is concerned this is not important, providing the model with the adjusted parameters gives the correct far field at all angle to the rotor axis. One measure of this, and the accuracy of the measurement, is that the results should be independent of the microphone array being used.

Figure 13 shows the beamformed and predicted levels for an array of 16 microphones that are furthest upstream from the rotor. The beamformed spectrum is seen to be about 3 dB higher across the whole spectrum than for the 51

microphone array, but the same is true for the prediction model, and the errors between the prediction and measurement are consistent for each array, giving confidence in the choice of the array and the prediction model.

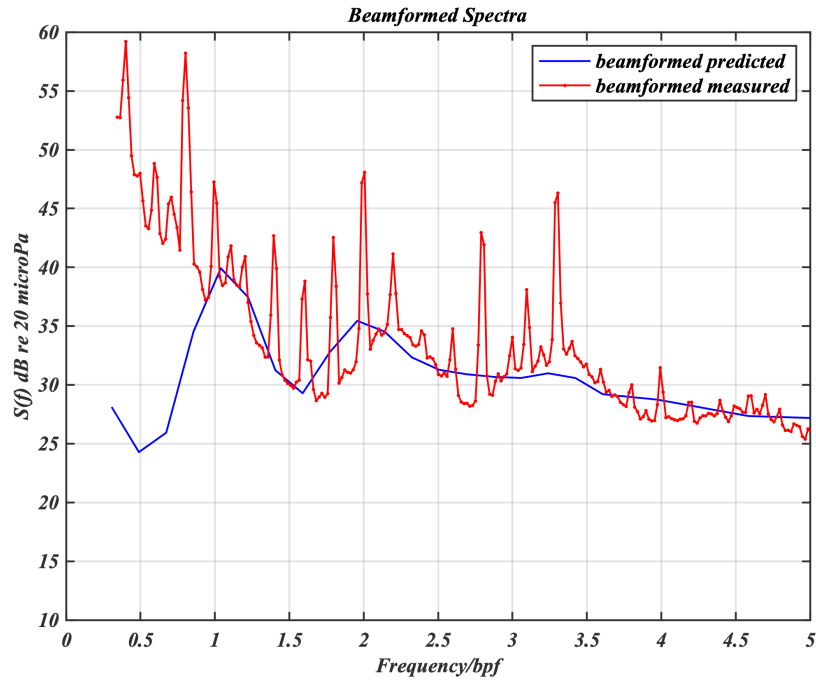


Figure 12: The beamformed spectral levels from the array microphones in the forward arc using delay and sum beamforming for array of 51 microphones.

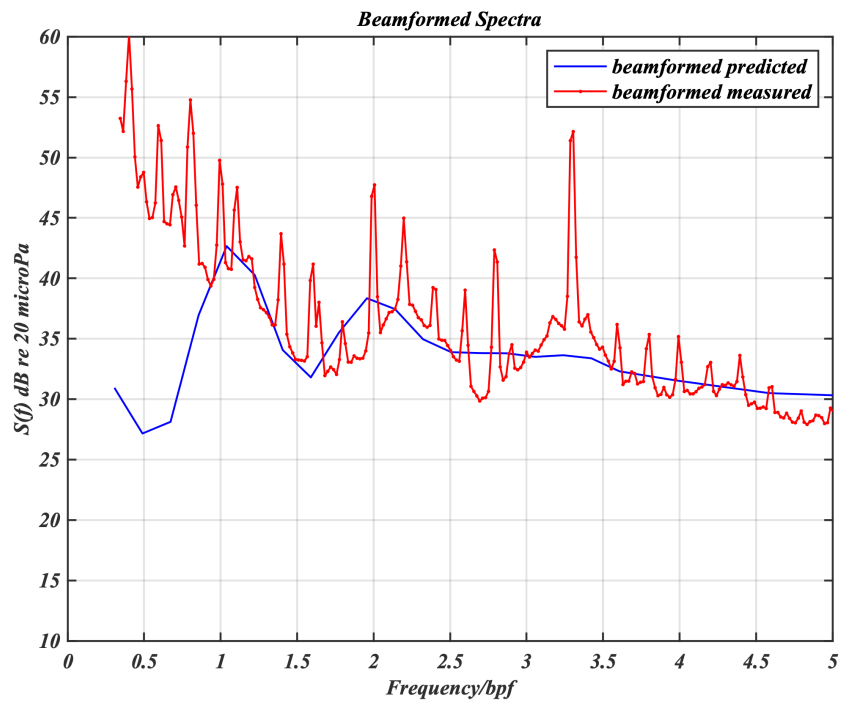


Figure 13: The beamformed spectral levels from the array microphones in the forward arc using delay and sum beamforming for array of 16 microphones.

V. Conclusion

In this paper we have considered the beamforming of rotor noise from a large microphone array in a wind tunnel and have shown how the array measurements for a single focus point can be compared with the levels predicted using a rotor noise prediction code. Using this approach it is found that the spectra agree at low frequencies, but there are discrepancies at high frequencies that may be the result of shear layer refraction by the wind tunnel walls. The results were found to be greatly improved if the turbulence correlation lengthscale was taken to be about twice the lengthscale measured by hot wires just upstream of the rotor in a separate test.

One of the key results of this study is that an alternative approach to measuring noise sources in high noise environments is given. The approach is not to focus on the source region and integrate a beamform map but rather to focus the array on the known source location and compare the array output to a model of the source. In the examples given here a sophisticated source model has been used, but in other application it may be possible to obtain results with a less sophisticated model. The key to this process is that knowledge about the acoustic source needs to be added to the beamforming process, and by doing so much more information about the source can be obtained than would be if it is modeled as an omni-directional point source.

VI. Acknowledgments

This work is supported by ONR grants numbers N00014-17-1-2682, N00014-20-1-2665 and N00014-17-1-2698. The authors would like to thank Dr. Ki-Han Kim and Dr. John Muench for their support of this project. In addition the authors would like to thank Dr. Brian Tester, Dr. William Blake and Dr. Jason Anderson for valuable discussion on this topic and inspiring many of the ideas presented.

III. References

- [1] Glegg, S., "Jet Noise Source Location", PhD Thesis, University of Southampton, 1979
- [2] Doherty, R., "Aeroacoustic Measurements", Mueller, (ed), Springer, 2002.
- [3] Fisher, M.J., Harper-Bourne, M., and Glegg, S.A.L., "Jet Engine Noise Source Location: The Polar Correlation Technique.", *Journal of Sound and Vibration*, Vol. 51(1), pp. 23-54, 1977.
- [4] Glegg, S.A.L., "The Accuracy of Source Distributions Measured by Using Polar Correlation", *Journal of Sound and Vibration*, Vol. 80(1) pp. 31-40, 1982
- [5] Hickling, C., Balantrapu, N.A., Millican, A., Alexander, W.N., Devenport, W.J., and Glegg, S.A.L., "Turbulence Ingestion into a Rotor at the Rear of an Axisymmetric Body" presented at the CEAS/AIAA Aeroacoustics Conference, Delft, The Netherlands, May 2019. AIAA paper no. 2019-2571
- [6] Glegg, S.A.L., Devenport, W.J., and Alexander, W.N., "Broadband rotor noise predictions using a time domain approach", *Journal of Sound and Vibration*, v. 335(2015) pp115–124
- [7] Glegg, S.A.L., Pectol, J., Devenport, W.J., and Alexander, W.N., "Benchmarking of a Broadband Rotor Noise Prediction Method", AIAA SciTech Conference, January 2018, Kissimmee, FL, AIAA Paper No: 2018-1005
- [8] Nicole Perry, "Noise Prediction Methods", MS Thesis, Florida Atlantic University, 2020
- [9] Glegg, S. and Devenport, W., "Aeroacoustics of Low Mach Number Flows", Academic Press, London, 2017